

MMNET: MUSCLE MOTION-GUIDED NETWORK FOR MICRO-EXPRESSION RECOGNITION

Hanting Li, Mingzhe Sui, Zhaoqing Zhu, Feng Zhao

University of Science and Technology of China, Hefei 230027, China
 {ab828658, sa20, zhaoqingzhu }@mail.ustc.edu.cn, {fzhao956}@ustc.edu.cn

ABSTRACT

Facial micro-expressions (MEs) are involuntary facial motions revealing peoples real feelings and play an important role in the early intervention of mental illness, the national security, and many human-computer interaction systems. However, existing micro-expression datasets are limited and usually pose some challenges for training good classifiers. To model the subtle facial muscle motions, we propose a robust micro-expression recognition (MER) framework, namely muscle motion-guided network (MMNet). Specifically, a continuous attention (CA) block is introduced to focus on modeling local subtle muscle motion patterns with little identity information, which is different from most previous methods that directly extract features from complete video frames with much identity information. Besides, we design a position calibration (PC) module based on the vision transformer. By adding the position embeddings of the face generated by PC module at the end of the two branches, the PC module can help to add position information to facial muscle motion pattern features for the MER. Extensive experiments on three public micro-expression datasets demonstrate that our approach outperforms state-of-the-art methods by a large margin.

1. INTRODUCTION

Facial expressions are an essential carrier for spreading human emotional information and coordinating interpersonal relationships. Most of the expressions we see in daily life are macro-expressions. However, spontaneous, brief, and subtle micro-expressions (MEs) can reveal peoples true feelings when people try to hide their real emotions under certain conditions [1], which makes MEs can be applied to many areas such as criminal interrogation, clinical diagnosis and human-computer interaction. Different from macro-expressions, MEs are usually accompanied by tiny facial muscle motions and last less than half a second (usually 1/25 to 1/3 second) [2], which makes micro-expression recognition (MER) task very difficult for humans, still more computers.

According to the features extraction methods, MER methods can be roughly divided into two categories: hand-crafted approaches and deep network-based approaches. For the former, histogram of oriented gradient (HOG), histogram of optical flow (HOOF) and local binary pattern-three orthogonal planes (LBP-TOP) are often used to extract MEs features. Le et al. learnt temporal and spectral structures with sparsity constraints by processing LBP-TOP [3]. Li et al. adopted the histogram of image gradient orientation-TOP (HIGO-TOP) for MER [4]. Happy et al. proposed a fuzzy-based HOOF (FHOOF) features extraction technique which only consider the muscle motion direction for MER [5]. However, due to the short duration and the inconspicuous motion of MEs, hand-craft features are often unable to robustly represent the differences between different micro-expressions, which is detrimental to MER.

In recent years, with the development of deep learning technology and the upgrading of computing hardware, more and more researchers have achieved promising results by designing different deep neural networks (DNNs) to handle MER tasks. Gan et al. introduced a novel features extractor that incorporates both the handcrafted (i.e., optical flow) and data-driven (i.e., convolutional neural networks (CNNs)) features [6]. Song et al. proposed a three-stream convolutional neural network (TSCNN) to recognize MEs by learning ME-discriminative features in three key frames of MEs videos [7]. Xie et al. introduced a novel MER approach by combining action units (AUs) and emotion category labels [8], while almost at the same time Lei et al. designed a graph temporal convolutional network (Graph-TCN) to extract the features of the local muscle motions of MEs. Xia et al. proposed a framework that leverages macro-expression samples as guidance for MER [9]. Among the latest results, Xia et al. designed a macro-to-micro transformation framework by two auxiliary tasks from spatial and temporal domain, respectively [10].

Although the above methods have gradually improved the performance of automated MER algorithms in recent years. Nevertheless, most of the them directly input the original video frames or the handcraft features of the video frames into DNNs to extract features of MEs, which makes DNNs easy to lead into the identity information of the samples. Obviously, identity information that has nothing to do with

The corresponding author is Feng Zhao

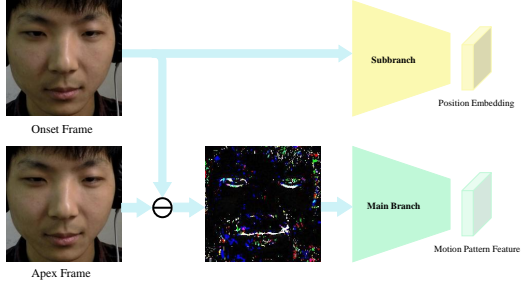


Fig. 1. The proposed two-branch MER paradigm.

expression is harmful to facial expression recognition (FER) task. This problem may have little impact on the macro-expression classification problem with abundant training data [11]. However, due to the extremely cost-consuming of collecting and labeling micro-expression data, we still do not have a large-scale micro-expression dataset comparable to the macro-expression datasets (e.g., AffectNet [12]). MEs are mainly determined by the position of facial muscle motion and the the muscle motion pattern (e.g., the slight upturn of the lips corner on both sides is likely to indicate happiness). So the key of MER is to learn the position and pattern of facial muscle motion rather than directly learn from entire video frame.

As shown in Figure 1, we propose a new two-branch MER paradigm to deal with the two key factors mentioned above, which extracts muscle motion pattern features from the difference between the onset frame and the apex frame through the main branch, and generates facial position embeddings from the onset frame only through the subbranch. We also give a specific realization of the proposed two-branch MER paradigm, namely muscle motion-guided network (MMNet), which mainly focus on learning the position (e.g., lips corner and upper eyebrow) and motion patterns (e.g., raise and lower) of facial muscle motions. Specifically, we learn the features of micro-expression video sequences by a two branch framework. First, we introduce a new continuous attention (CA) block to learn the patterns of facial muscle motion. CA block can pay attention to the location of the motion and extract features related to motion patterns. Second, we devise a position calibration (PC) module based on vision transformer (ViT) [13] to add robust facial position information to the learned motion pattern features. It should be noted that the main branch of MMNet only models the difference between the onset frame and the apex frame, which makes the model less affected by the identity information.

The contributions of our work are summarized as follows:

- We propose a novel two-branch MER paradigm, which extracts muscle motion pattern features and facial position embeddings through the main branch and subbranch, respectively. Then the two kinds of features are fused at the end of the network for classification.

- We devise a muscle motion-guided network (MMNet) to implement the above-mentioned two-branch MER paradigm. The main branch for extracting the motion pattern features is composed of the proposed continuous attention (CA) block and the subbranch to extract the position features is realized through our designed position calibration (PC) module.
- Our MMNet outperforms state-of-the-art approaches by a large margin on three popular micro-expression datasets (i.e. CASME II, SAMM and MMEW). Extensive experiments demonstrate the effectiveness of our proposed two-branch MER paradigm.

2. METHOD

In this section, we detail the two branches of our proposed MMNet for MER. First, we explain the motivation for proposing the new two-branch MER paradigm and give an overview of the proposed MMNet. Then we describe the details of the continuous attention block and position calibration module which constitute the two branches of MMNet.

2.1. Problem Formulation & Overview

Existing MER methods often focus on designing the structures of deep networks to improve the recognition accuracy, but often neglect to find better ways to utilize the video frames of MEs. Most approaches input the original video frames with identity information into a single-branch network [14, 15], or extract handcraft features (e.g., optical flow or LBP) from the frames and then fuse them by a multi-branch network [16]. Since the input for the main branch contains the identity information of the sample to varying degrees, the network is likely to learn identity related features that has nothing to do with MER tasks, especially when MEs data is insufficient. To tackle this problem, we raise a novel two-branch MER paradigm. The main branch is proposed to deal with the motion pattern, and the lightweight subbranch extract facial position embeddings from the onset frame which mainly contains the facial position information without any expression related information. In this way, even if the onset frame contains certain identity information, since it is only fed into the lightweight subbranch, the whole network can still focus on learning the motion pattern rather than identity.

As seen in Figure 2, our proposed MMNet mainly consists of two branches. The main branch extracts the motion pattern features with the difference between the apex frame and the onset frame as input, and the subbranch is used to generate the facial position embeddings with low resolution onset frame as the input. Finally, the facial position embeddings are added to the motion pattern features for mapping the motion pattern to specific face areas.

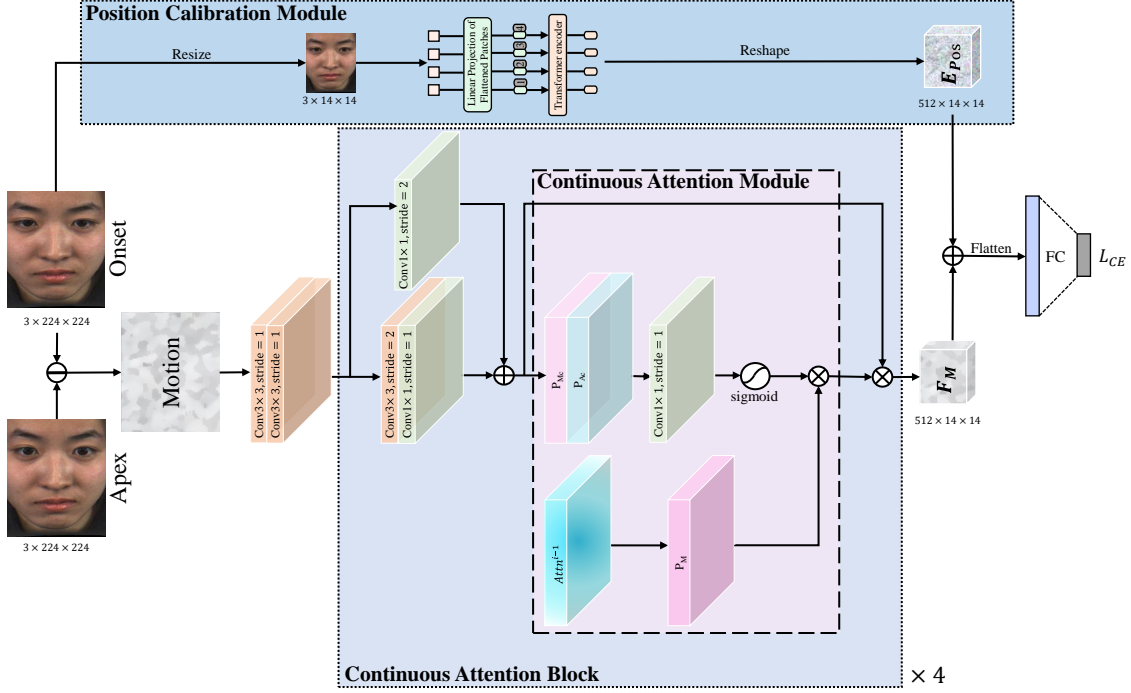


Fig. 2. The pipeline of the MMNet. It contains two branches: continuous attention block to extract motion pattern features and position calibration module to locate the specific location of muscle motion. Here, L_{CE} stands for the cross-entropy loss function.

2.2. Continuous Attention Block

Compared with macro expressions, MEs tend to have smaller muscle motions and more local active areas, which makes it difficult for the traditional attention modules to accurately focus on the subtle facial muscle motions. To solve it, some works tried to model the relationship between muscle motions and MEs [8] with the help of action units (AUs) labels [17]. However, it is still a huge challenge to obtain precise attention maps without introducing extra supervision.

To solve this, we devise a continuous attention block by introducing the attention maps of the previous layer as the prior knowledge of the attention maps of the current layer. Inspired by the convolutional block attention (CBAM) module [18] depicted in Figure 3(a), we utilize both max-pooling outputs and average-pooling outputs to calculate the spatial attention maps. As shown in Figure 3(b), we make the attention maps of the previous layer as the prior knowledge to obtain the attention maps of the current layer, and use a smaller convolution kernel (i.e., 1×1) to obtain more local attention maps. Formally, the CA module can be defined as,

$$\begin{aligned} Attn^i &= M^i(F_{conv}^i, Attn^{i-1}) \\ &= \sigma(f_{1 \times 1}^i([P_{Mc}(F_{conv}^i); P_{Ac}(F_{conv}^i)])) \otimes P_M(Attn^{i-1}), \end{aligned} \quad (1)$$

with

$$F_{conv}^i = f_{1 \times 1}^i(f_{3 \times 3}^i(F^i)) + f_{1 \times 1}^i(F^i), \quad (2)$$

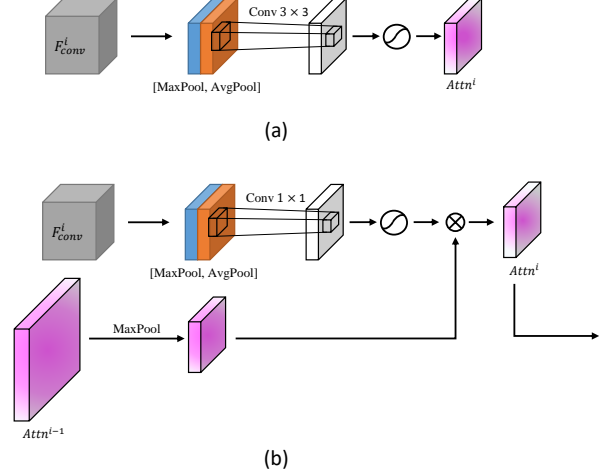


Fig. 3. Diagram of CBAM module and CA module: (a) CBAM module (b) our CA module.

where M^i is the CA module of the i^{th} CA block that expects to pay attention to the muscle motion areas and $Attn^{i-1}$ is the attention maps of the $(i-1)^{th}$ layer. $F_{conv}^i \in \mathbb{R}^{2C \times H \times W}$ denotes the features extracted by the first two convolutional layers of the i^{th} layer as the input of CA module. σ denotes the sigmoid function. $f_{1 \times 1}^i$ and $f_{3 \times 3}^i$ represent a convolution operation with the filter size of 1×1 and 3×3

from the i^{th} layer, respectively. $P_{Mc}(F_{conv}^i) \in \mathbb{R}^{1 \times H \times W}$ and $P_{Ac}(F_{conv}^i) \in \mathbb{R}^{1 \times H \times W}$ stand for max-pooled features and average-pooled features across the channel, respectively. P_M represents the max-pooling operation on the attention maps of $(i-1)^{th}$ layer to match the size of current layer attention maps, while \otimes means the element-wise product for introducing the attention maps from last layer $Attn^{i-1}$ as prior knowledge. $F^i \in \mathbb{R}^{C \times 2H \times 2W}$ stands for the input of the i^{th} CA block.

By associating the attention mechanism between adjacent layers, the CA block can gradually and robustly focus on the areas that have subtle motions, instead of focusing on different areas of the face in different layers, which make networks to learn both MEs related areas and unrelated areas. We use four CA blocks to constitute the main branch of the MMNet to learn the subtle muscle motion pattern F_M with the size of $512 \times 14 \times 14$. The CA block which consists of the CA module and two convolutional layers can be formulated as,

$$CA(F^i, Attn^{i-1}) = F_{conv}^i \otimes M^i(F_{conv}^i, Attn^{i-1}), \quad (3)$$

where CA represents the proposed continuous attention block and, \otimes stands for broadcast element-wise multiplication, which means each channel of $F_{conv}^i \in \mathbb{R}^{2C \times H \times W}$ will be multiplied by the spatial attention maps $M^i(F_{conv}^i, Attn^{i-1}) \in \mathbb{R}^{1 \times H \times W}$ to pay attention to the region of interest. The ablation experiments and visualization in Figure 4 demonstrate that our CA block can help to pay attention to accurate MEs related areas. As shown in Figure 2, we take the difference between the apex frame and the onset frame as the input of the main branch to learn the motion pattern features.

2.3. Position Calibration Module

Due to the various appearance of different people in the micro-expression datasets, it is hard to strictly align all the faces because of various interpupillary distances, different nose sizes, etc. Therefore, the same face areas may correspond to different pixel position of the image, which make it hard for the network to learn exactly where the subtle motion occurs. In order to accurately add position information to the motion pattern features extracted from the main branch, we propose a position calibration module as the subbranch of MMNet to generate a facial position embeddings for mapping motion pattern features to specific areas of the face.

Since the relative positions of the facial features are basically determined (e.g., the nose is usually located below the middle of the two eyes), modeling long-distance dependencies can effectively help locate the positions of various parts of the face and generate robust position embeddings. Recently, ViT has used self-attention mechanism to model long-distance dependencies and has achieved promising results on image classification tasks, while the convolutional

Table 1. Summary of the data distributions for CASME II (five classes) and SAMM (five classes) and MMEW (four classes).

Label \ Dataset	SAMM	CSAME II	MMEW
Happiness	26	32	36
Anger	57	—	—
Contempt	12	—	—
Disgust	—	63	72
Repression	—	27	—
Surprise	15	28	89
Others	26	99	66
Total	136	249	263

Table 2. Summary of the data distributions for CASME II (three classes) and SAMM (three classes).

Label \ Dataset	SAMM	CSAME2
Positive	26	32
Negative	92	96
Surprise	15	28
Total	133	156

neural networks (CNNs) often needs many convolutional layers to obtain a global receptive field, which is not conducive to modeling facial position information. So we introduce the PC module based on a shallow ViT. As shown in Figure 2, we utilize the difference between the apex frame and the onset frame to learn the motion related features F_M and the onset frame to learn the facial position embeddings E_{pos} . Since we only need to learn the location of important face landmarks (e.g., the location of eyes, mouth and nose), not the detailed texture related to the identity of samples (e.g., wrinkles and skin tone), we scale the onset frame to the same size of 14×14 as the input of subbranch matching the size of F_M . Then we reshape the scaled onset frame into a sequence of 196 flattened 2D patches I_p with the size of $1 \times 1 \times 3$ then map them through a trainable linear projection to get patch embeddings E_p with 512 dimensions, which matches the channel dimension of F_M . After adding the position embeddings of ViT to retain position information as done in [13], these patch embeddings are sent to transformer encoder to learn the relationship between patches. Finally, the output of ViT with the size of 196×512 is reshaped to $512 \times 14 \times 14$ to get E_{pos} for position calibration. The position embeddings E_{pos} are then added to the motion pattern features F_M for mapping the motion pattern to specific face areas for MER.

3. EXPERIMENT

To verify the effectiveness of MMNet, we conduct extensive experiments on three popular micro-expression datasets (i.e.,

CASME II [19], SAMM [20] and MMEW [21]). In this section, we first introduce these three datasets used in our experiments and implementation details. Then we explore the performance of two branches of MMNet on these datasets, respectively. Subsequently, we compare our method with several state-of-the-art approaches.

3.1. Datasets

CASME II [19] contains 256 micro-expression videos from 26 subjects with the cropped sizes of 280×340 at 200 fps. Consistent with most of previous methods, only samples of five prototypical expressions, i.e., happiness, disgust, repression, surprise, and others, are used. **SAMM** [20] has 159 micro-expression clips from 32 participants from 13 different ethnicities at 200 fps. Consistent with most of the previous work, happiness, anger, contempt, surprise, and others expressions are utilized for experiments. **MMEW** [21] contains both macro and micro-expressions sampled from the same subjects for researchers to explore the relationship between them. It contains 300 MEs and 900 macro-expression samples with a larger resolution (1920×1080) at 90 fps. We use happiness, surprise, disgust and others expressions for ablation study. Table 1 shows the dataset distributions for each expression class for CASME II (five classes) and SAMM (five classes) and MMEW (four classes), while Table 2 shows the dataset distributions for each expression class for CASME II (three classes) and SAMM (three classes).

First, we conduct ablation studies on CASME II, SAMM and MMEW datasets separately to verify the effectiveness of the proposed CA block and PC module. The accuracy and F1-score are used for evaluation. Second, since the MMEW dataset has just been proposed in 2021, there is currently few methods for comparison on this benchmark. So we mainly compare MMNet with with other state-of-the-art approaches on CASME II and SAMM datasets. Consistent with most of the previous work, leave-one-subject-out (LOSO) cross-validation is used in all experiments, which means every subject is taken as a test set in turn and the other subjects as the training data. For all the experiments, the accuracy and F1-score are used for evaluations.

3.2. Implementation Details

In our experiments, we use *Dlib* software to detect the landmark points on the face and crop the images according to these landmark points. The cropped images on all the datasets are resized to the size of 224×224 . To avoid over-fitting, we randomly pick a frame from four frames around the labeled onset and apex frame as the onset and apex frame for training. The horizontal flipping, random cropping and color jittering are also employed. We use four CA blocks to constitute the main branch and a shallow ViT to build the subbranch of MMNet. In the training stage, we adopt AdamW to optimize our MMNet with a batch size of 32. The learning rate is initialized

to 0.0008, decreased at an exponential rate in 70 epochs for cross-entropy loss function. For fair comparison, we set the number of self-attention heads N_H and the number of transformer encoder layers N_L to 4 and 2 by default, respectively. All the experiments are conducted on a single NVIDIA RTX 3070 card with Pytorch toolbox.

3.3. Ablation Studies

Effectiveness of Two Branches in MMNet. To verify our CA block and PC module, we set a ResNet consisting of four building blocks which is used in ResNet18 [22] as the baseline model for ablation study. Then we separately replace the building blocks of ResNet18 with the CA block and add the PC module to compare the proved model with the baseline on three datasets. As shown in Table 3, the proposed CA block and PC module both can significantly improve the performance. Finally, when we use both the modules to build our MMNet, the result exceeds the baselines by 7.23%, 6.61%, and 5.70% on CASME II, SAMM and MMEW datasets, respectively, which fully indicates the importance and effectiveness of two branches in MMNet.

Comparisons between Continuous Attention and Independent Attention. To illustrate the effectiveness of introducing attention maps of the previous layers as prior knowledge on the MER task, we compare the proposed continuous attention module with traditional attention module, which generate attention maps independently in each layer. It should be noted that both settings add the PC module to generate the position embeddings. As shown in Table 4, the performance of continuous attention module on the three datasets are significantly better than independent attention module, which illustrates the importance of getting precise attention maps on the MER task.

Impact of the number of layers and heads of PC module. Vision transformer encoder consists of N_L identical layers. The multi-head self-attention in each layer enables the model decomposes the information into N_H representation subspaces and jointly capture discriminative information at different positions. We explore the effects of different layer values N_L and the number of heads N_H on CASME II and SAMM datasets. Table 5 shows the comparison of performance of different hyper-parameter settings of our method. We observe that smaller N_H and N_L tend to achieve better results. We think this is because that larger models being are more prone to overfitting. So we set the number of self-attention heads N_H and the number of transformer encoder layers N_L to 2 and 4 when comparing our MMNet with other state-of-the-art approaches.

3.4. Comparison with State-of-the-arts

We also compare our MMNet with several state-of-the-art methods. From Table 6 and 7, we can see that our

Table 3. Evaluation of the continuous attention block and position calibration module.

Method	CASME2 (5 classes)		SAMM (5 classes)		MMEW (4 classes)	
	Accuracy (%)	F1-Score	Accuracy (%)	F1-Score	Accuracy (%)	F1-Score
Baseline(ResNet)	81.12	0.7582	73.53	0.6345	81.75	0.7921
CA block	83.13	0.7891	76.47	0.6593	84.03	0.8206
PC module	85.14	0.8362	77.21	0.6734	85.55	0.8402
PC module + CA block	88.35	0.8676	80.14	0.7291	87.45	0.8635

Table 4. Comparison of continuous attention module and independent attention module. The best results are in bold.

Method	CASME2 (5 classes)		SAMM (5 classes)		MMEW (4 classes)	
	Accuracy (%)	F1-Score	Accuracy (%)	F1-Score	Accuracy (%)	F1-Score
Independent attention	84.74	0.8216	77.21	0.7000	80.99	0.7941
Continuous attention	88.35	0.8676	80.14	0.7291	87.45	0.8635

Table 5. Ablation study w.r.t. number of heads, number of layers, performed on CSAME2 (5 classes) and SAMM (5 classes). N_L represent the number of ViT encoder and N_H stands for number of heads. Bold values correspond to better performance.

Setting	N_L	N_H	CSAME2 (%)	SAMM (%)
i	2	2	86.35	79.41
ii	2	4	88.35	80.14
iii	2	8	85.94	78.68
iv	3	2	84.74	80.88
v	3	4	85.94	80.14
vi	3	8	84.34	76.47

MMNet outperforms the best results of previous methods on every evaluation indicators. Specifically for three classes MER tasks, our method outperforms GACNN [23] by 1.5%/2.73% and 5.85%/7.99% on SAMM and CASME II of of accuracy/F1-score, respectively. As for five classes, our MMNet exceeds SMA-STN [26] by 2.94%/2.58% and 5.76%/7.3% on SAMM and CASME II of of accuracy/F1-score, respectively. The result fully demonstrate the superiority of the MMNet based on the proposed two-branch MER paradigm.

3.5. Visualization

In order to prove that our proposed continuous attention module can pay attention to the movements of tiny facial muscles, we visualize some attention maps of the first CA block in Figure 4. We can see that CA module can generate attention maps to help the network pay attention to where the facial muscle moves. Specifically, CA module pay attention to the upper end of the eyebrows for surprise samples and the corner of the mouth for happiness samples.

Table 6. Comparison results on CASME II dataset. Cate stands for the number of the classes. The highest accuracy is highlighted in bold.

Method	Protocol	cate	Acc (%)	F1-Score
OFF-ApexNet [6]	LOSO	3	88.28	0.8697
STSTNet [16]	LOSO	3	86.86	0.8382
AU-GACN [8]	LOSO	3	71.20	0.3550
MTMNet [9]	LOSO	3	75.60	0.7010
MiNet&MaNet [10]	LOSO	3	79.90	0.7590
GACNN [23]	LOSO	3	89.66	0.8695
DSSN [24]	LOSO	5	71.19	0.7297
TSCNN [7]	LOSO	5	80.97	0.8070
Dynamic [25]	LOSO	5	72.61	0.6700
Graph-TCN [15]	LOSO	5	73.98	0.7246
SMA-STN [26]	LOSO	5	82.59	0.7946
AU-GCN [27]	LOSO	5	74.27	0.7047
GEME [28]	LOSO	5	75.20	0.7354
MERSiamC3D [29]	LOSO	5	81.89	0.8300
MMNet (Ours)	LOSO	3	95.51	0.9494
MMNet (Ours)	LOSO	5	88.35	0.8676

4. CONCLUSION

In this paper, we propose a new two-branch MER paradigm and give a realization of the new paradigm called MMNet. Specifically, the main branch based on the proposed CA block focuses on learning motion pattern features from the difference between the onset frame and the apex frame, while the subbranch based on PC module focuses on generating position embeddings for position calibration. Experiments illustrate that our MMNet outperforms state-of-the-art methods by a large margin on CASME II and SAMM datasets.

Table 7. Comparison results on SAMM dataset. Cate stands for the number of the classes. The best accuracy is highlighted in bold.

Method	Protocol	cate	Acc (%)	F1-Score
OFF-ApexNet [6]	LOSO	3	68.18	0.5423
STSTNet [16]	LOSO	3	68.10	0.6588
AU-GACN [8]	LOSO	3	70.2	0.4330
MTMNet [9]	LOSO	3	74.10	0.7360
MiNet&MaNet [10]	LOSO	3	76.70	0.7640
GACNN [23]	LOSO	3	88.72	0.8118
DSSN [24]	LOSO	5	57.35	0.4644
Graph-TCN [15]	LOSO	5	75.00	0.6985
SMA-STN [26]	LOSO	5	77.20	0.7033
AU-GCN [27]	LOSO	5	74.26	0.7045
GEME [28]	LOSO	5	55.38	0.4538
MERSiamC3D [29]	LOSO	5	68.75	0.6400
MMNet (Ours)	LOSO	3	90.22	0.8391
MMNet (Ours)	LOSO	5	80.14	0.7291

References

- [1] P. Ekman, *Telling lies: Clues to deceit in the marketplace, politics, and marriage (revised edition)*, WW Norton & Company, 2009.
- [2] P. Ekman and W. Friesen, “Constants across cultures in the face and emotion,” *Journal of personality and social psychology*, vol. 17, no. 2, pp. 124, 1971.
- [3] A. Le Ngo and J. See and R. Phan, “Sparsity in dynamics of spontaneous subtle emotions: Analysis and application,” *IEEE TAC*, vol. 8, no. 3, pp. 396–411, 2016.
- [4] X. Li, X. Hong, A. Moilanen, X. Huang, T. Pfister, G. Zhao, and M. Pietikäinen, “Towards reading hidden emotions: A comparative study of spontaneous micro-expression spotting and recognition methods,” *IEEE TAC*, vol. 9, no. 4, pp. 563–577, 2017.
- [5] S. Happy and A. Routray, “Fuzzy histogram of optical flow orientations for micro-expression recognition,” *IEEE TAC*, vol. 10, no. 3, pp. 394–406, 2017.
- [6] Y. Gan, S. Liang, W. Yau, Y. Huang, and L. Tan, “OFF-ApexNet on micro-expression recognition system,” *Signal Processing: Image Communication*, vol. 74, pp. 129–139, 2019.
- [7] B. Song, K. Li, Y. Zong, J. Zhu, W. Zheng, J. Shi, and L. Zhao, “Recognizing spontaneous micro-expression using a three-stream convolutional neural network,” *IEEE Access*, vol. 7, pp. 184537–184551, 2019.
- [8] H. Xie, L. Lo, H. Shuai, and W. Cheng, “Au-assisted graph attention convolutional network for micro-expression recognition,” in *MM*, 2020, pp. 2871–2880.
- [9] B. Xia, W. Wang, S. Wang, and E. Chen, “Learning from macro-expression: A micro-expression recognition framework,” in *MM*, 2020, p. 2936–2944, Association for Computing Machinery.
- [10] B. Xia and S. Wang, “Micro-expression recognition enhanced by macro-expression from spatial-temporal domain,” *IJCAI*, 2021.
- [11] S. Li and W. Deng, “Deep facial expression recognition: A survey,” *IEEE TAC*, 2020.
- [12] A. Mollahosseini, B. Hasani, and M. Mahoor, “Affectnet: A database for facial expression, valence, and arousal computing in the wild,” *IEEE TAC*, vol. 10, no. 1, pp. 18–31, 2017.
- [13] A. Dosovitskiy, L. Beyer, A. Kolesnikov, D. Weissenborn, X. Zhai, T. Unterthiner, M. Dehghani, M. Minderer, G. Heigold, S. Gelly, et al., “An image is worth 16x16 words: Transformers for image recognition at scale,” *arXiv preprint arXiv:2010.11929*, 2020.
- [14] Y. Li, X. Huang, and G. Zhao, “Joint local and global information learning with single apex frame detection for micro-expression recognition,” *IEEE TIP*, vol. 30, pp. 249–263, 2020.
- [15] L. Lei, J. Li, T. Chen, and S. Li, “A novel Graph-TCN with a graph structured representation for micro-expression recognition,” in *MM*, 2020, pp. 2237–2245.
- [16] S. Liang, Y. Gan, J. See, H. Khor, and Y. Huang, “Shallow triple stream three-dimensional CNN (STSTNet)

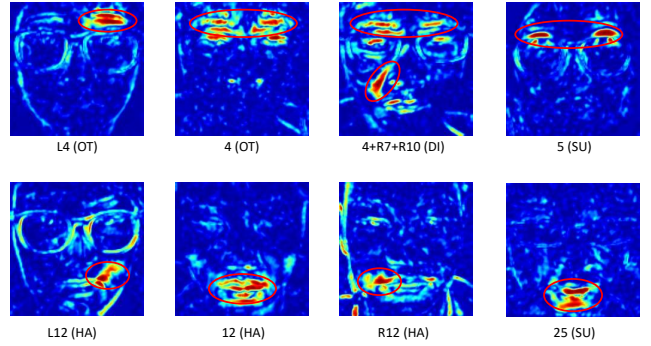


Fig. 4. Visualization of the attention maps of several samples from MMEW dataset. The outside brackets represent action units label of the samples (e.g., L12 stands for the left corner of the lips and R12 represent the right corner of the lips.), while the label inside the brackets is the label of expression type (e.g., SU, HA, DI, and OT represent surprise, happiness, disgust, and others, respectively).

for micro-expression recognition,” in *FG*. IEEE, 2019, pp. 1–5.

[17] E. Friesen and P. Ekman, “Facial action coding system: a technique for the measurement of facial movement,” *Palo Alto*, vol. 3, no. 2, pp. 5, 1978.

[18] S. Woo, J. Park, J. Lee, and I. Kweon, “CBAM: Convolutional block attention module,” in *ECCV*, 2018, pp. 3–19.

[19] W. Yan, X. Li, S. Wang, G. Zhao, Y. Liu, Y. Chen, and X. Fu, “CASME II: An improved spontaneous micro-expression database and the baseline evaluation,” *PLoS one*, vol. 9, no. 1, pp. e86041, 2014.

[20] A. Davison, C. Lansley, N. Costen, K. Tan, and M. Yap, “SAMM: A spontaneous micro-facial movement dataset,” *IEEE TAC*, vol. 9, no. 1, pp. 116–129, 2016.

[21] X. Ben, Y. Ren, J. Zhang, S. Wang, K. Kpalma, W. Meng, and Y. Liu, “Video-based facial micro-expression analysis: A survey of datasets, features and algorithms,” *IEEE TPAMI*, 2021.

[22] K. He, X. Zhang, S. Ren, and J. Sun, “Deep residual learning for image recognition,” in *CVPR*, 2016, pp. 770–778.

[23] A. Kumar and B. Bhanu, “Micro-expression classification based on landmark relations with graph attention convolutional network,” in *CVPRW*, 2021, pp. 1511–1520.

[24] H. Khor, J. See, S. Liong, R. Phan, and W. Lin, “Dual-stream shallow networks for facial micro-expression recognition,” in *ICIP*. IEEE, 2019, pp. 36–40.

[25] B. Sun, S. Cao, D. Li, J. He, and L. Yu, “Dynamic micro-expression recognition using knowledge distillation,” *IEEE TAC*, 2020.

[26] J. Liu, W. Zheng, and Y. Zong, “SMA-STN: Segmented movement-attending spatiotemporal network for micro-expression recognition,” *arXiv preprint arXiv:2010.09342*, 2020.

[27] L. Lei, T. Chen, S. Li, and J. Li, “Micro-expression recognition based on facial graph representation learning and facial action unit fusion,” in *CVPRW*, 2021, pp. 1571–1580.

[28] X. Nie, M. Takalkar, M. Duan, H. Zhang, and M. Xu, “GEME: Dual-stream multi-task gender-based micro-expression recognition,” *Neurocomputing*, vol. 427, pp. 13–28, 2021.

[29] S. Zhao, H. Tao, Y. Zhang, T. Xu, K. Zhang, Z. Hao, and E. Chen, “A two-stage 3D CNN based learning method for spontaneous micro-expression recognition,” *Neurocomputing*, vol. 448, pp. 276–289, 2021.